SUPPLEMENTARY INFORMATION

GLP-catalyzed H4K16me1 promotes 53BP1 recruitment to permit DNA damage repair and cell survival

Xiaopeng Lu†, Ming Tang†, Qian Zhu, Qiaoyan Yang, Zhiming Li, Yantao Bao, Ge Liu, Tianyun Hou, Yafei Lv, Ying Zhao, Haiying Wang, Yang Yang, Zhongyi Cheng, He Wen, Baohua Liu, Xingzhi Xu, Luo Gu, and Wei-Guo Zhu

†These authors contributed equally to this paper.

Supplementary Information

Supplementary Figures S1 to S8
Supplementary Table S1

Figure S1

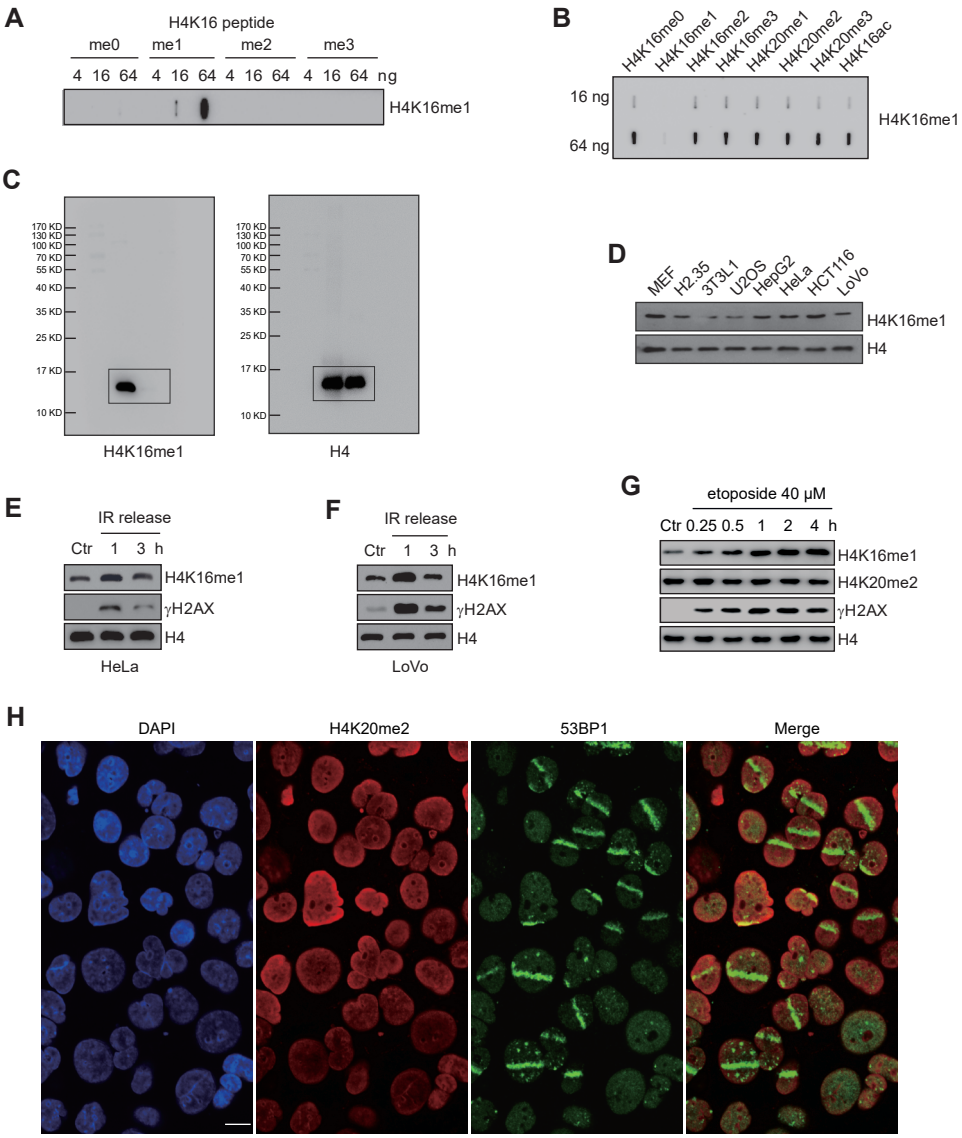
A
H4K16 peptide
me0
me1
me2
me3
4 16 64 4 16 64 4 16 64 4 16 64 ng
H4K16me1
B
H4K16me0
H4K16me1
H4K16me2
H4K16me3
H4K20me1
H4K20me2
H4K20me3
H4K16ac
16 ng
64 ng
H4K16me1
C
170 KD
130 KD
100 KD
70 KD
55 KD
40 KD
35 KD
25 KD
17 KD
10 KD
H4K16me1
H4
D
MEF
H2.35
3T3L1
U2OS
HepG2
HeLa
HCT116
LoVo
H4K16me1
H4
E
IR release
Ctr 1 3 h
H4K16me1
γH2AX
H4
HeLa
F
IR release
Ctr 1 3 h
H4K16me1
γH2AX
H4
LoVo
G
etoposide 40 μM
Ctr 0.25 0.5 1 2 4 h
H4K16me1
H4K20me2
γH2AX
H4
H
DAPI
H4K20me2
53BP1
Merge

Figure S1. H4K16me1 increases in response to DNA damage.

(A) Slot blot assay showing the high specificity of the H4K16me1 antibody. Cross reactivity with peptides carrying other modifications was not detected.

(B) Peptide competition assay showing that only pre-incubation of H4K16me1 peptide with H4K16me1 antibody efficiently blocks H4K16me1 epitope recognition.

(C) H4K16me1 expression was detected in HEK293 cells. Recombinant Histone H4 (rH4) was used as a negative control. The entire western blot membranes probed in parallel with H4K16me1 and H4 were shown. The blots in the frames were used in Figure 1B.

(D) H4K16me1 expression in different mammalian cell lines.

(E, F) HeLa and LoVo cells were exposed to 10 Gy X-ray irradiation and then re-cultured for 1 h or 3 h in fresh medium. Histones were extracted for western blotting.

(G) HCT116 cells were treated with 40 μM etoposide for the indicated time. Histones were extracted for western blotting.

(H) HeLa cells were micro-irradiated as previously described. After 10 min, cells were washed, fixed and stained with anti-H4K20me2 and anti-53BP1 antibodies. Similar results were obtained from three independent experiments. Scale bars: 10 μm.

Figure S2

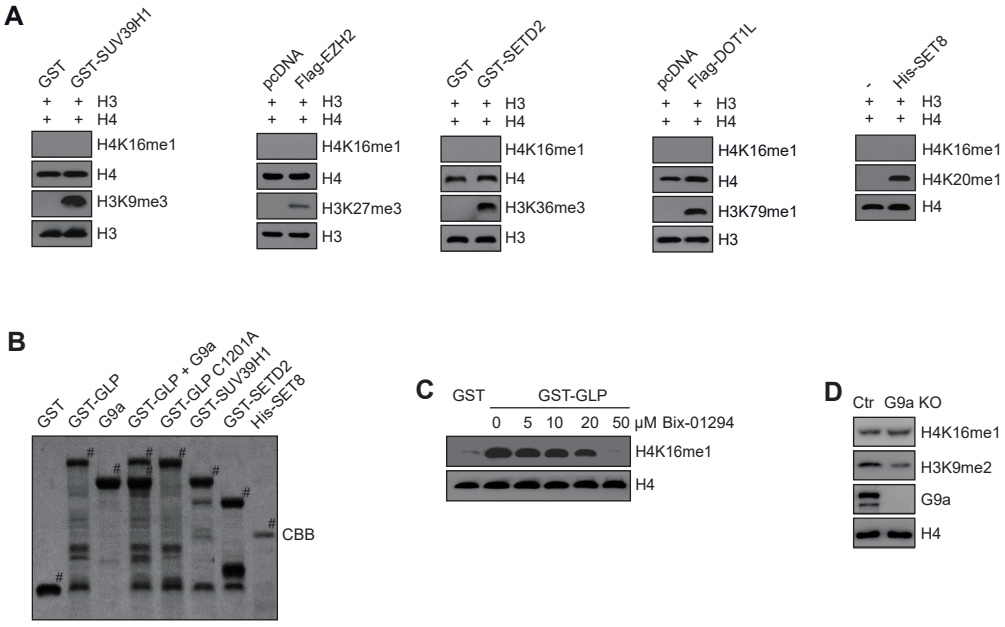
A
GST
GST-SUV39H1
+ + H3
+ + H4
H4K16me1
H4
H3K9me3
H3
pcDNA
Flag-EZH2
+ + H3
+ + H4
H4K16me1
H4
H3K27me3
H3
GST
GST-SETD2
+ + H3
+ + H4
H4K16me1
H4
H3K36me3
H3
pcDNA
Flag-DOT1L
+ + H3
+ + H4
H4K16me1
H4
H3K79me1
H3
His-SET8
+ + H3
+ + H4
H4K16me1
H4K20me1
H4
B
GST
GST-GLP
G9a
GST-GLP + G9a
GST-GLP C1201A
GST-SUV39H1
GST-SETD2
His-SET8
CBB
C
GST
GST-GLP
0 5 10 20 50 μM Bix-01294
H4K16me1
H4
D
Ctr
G9a KO
H4K16me1
H3K9me2
G9a
H4

Figure S2. GLP catalyzes H4K16me1 both *in vitro* and *in vivo*.

(A) *In vitro* methylation assays were performed using different methyltransferases. Recombinant histones H3 and H4 were used as substrates.

(B) Coomassie brilliant blue staining of the methyltransferases used in Figure 2B, indicated with "#".

(C) Recombinant H4 (2 μg) was incubated with GST or GST-GLP in methylation reaction buffer with increasing concentrations of Bix-01294. Samples were then analyzed by western blotting.

(D) H4K16me1, H3K9me2, G9a and histone H4 expression levels in G9a knockout (KO) HCT116 cells.

Figure S3

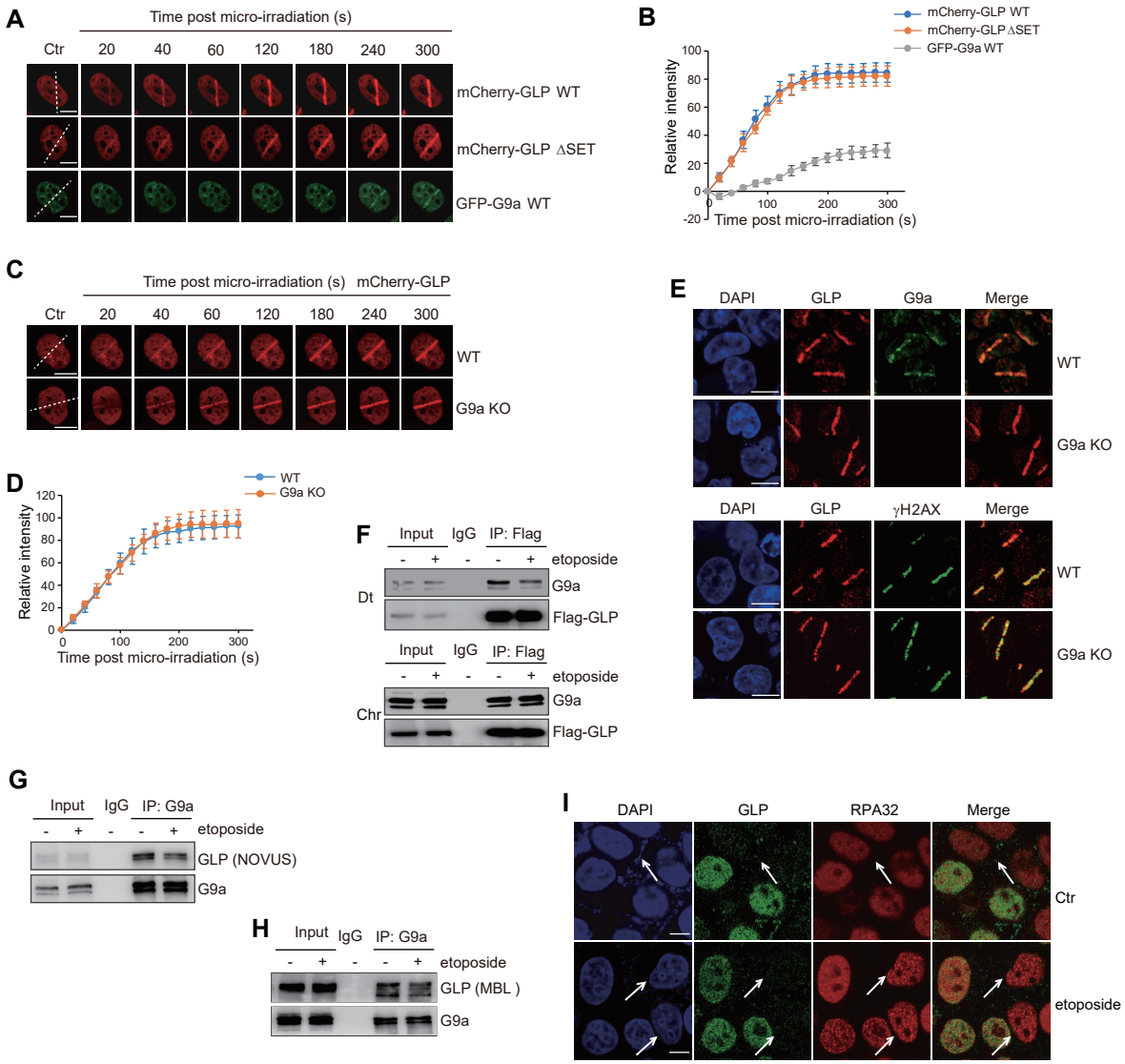
A
Time post micro-irradiation (s)
Ctr
20
40
60
120
180
240
300
mCherry-GLP WT
mCherry-GLP ΔSET
GFP-G9a WT
B
mCherry-GLP WT
mCherry-GLPΔSET
GFP-G9a WT
Relative intensity
Time post micro-irradiation (s)
C
Time post micro-irradiation (s)
mCherry-GLP
WT
G9a KO
D
WT
G9a KO
Relative intensity
Time post micro-irradiation (s)
E
DAPI
GLP
G9a
Merge
WT
G9a KO
DAPI
GLP
γH2AX
Merge
WT
G9a KO
F
Input
IgG
IP: Flag
etoposide
Dt
G9a
Flag-GLP
Chr
G
Input
IgG
IP: G9a
etoposide
GLP (NOVUS)
G9a
H
Input
IgG
IP: G9a
etoposide
GLP (MBL)
G9a
I
DAPI
GLP
RPA32
Merge
Ctr
etoposide

Figure S3. GLP has different roles to G9a in the DNA damage response.

(A) Dynamics of mCherry-GLP (WT), mCherry-GLP (ΔSET) or GFP-G9a at micro-irradiated sites (indicated by a broken white line) in HeLa cells. Consistent results were observed in three different experiments. Scale bars: 10 μm.

(B) Relative intensities of mCherry-GLP (WT), mCherry-GLP (ΔSET) or GFP-G9a at micro-irradiated sites in the experiment described in A. The data represent the means ±SD.

(C) Dynamics of mCherry-GLP at micro-irradiated sites (indicated by a broken white line) in HCT116 WT and HCT116 G9a KO cells. Consistent results were observed in three different experiments. Scale bars: 10 μm.

(D) Relative intensities of mCherry-GLP at micro-irradiated sites in the experiment described in C. The data represent the means ±SD.

(E) HCT116 WT and HCT116 G9a KO cells were micro-irradiated and fixed 10 min later for immunostaining with the indicated antibodies. Scale bars: 10 μm.

(F) Soluble (Dt) and chromatin fractions (Chr) extracted from HCT116 cells were immunoprecipitated with anti-Flag M2 beads and probed with the indicated antibodies.

(G, H) HCT116 cells were treated with 40 μM etoposide for 30 min before drug withdrawal. After re-culture for 30 min, cells were collected and the Dt fraction was used for anti-G9a immunoprecipitation. For (G), anti-G9a (Sigma) and anti-GLP (NOVUS) antibodies were used; for (H), anti-G9a (Sigma) and anti-GLP (MBL) antibodies were used.

(I) shCtr and shGLP HeLa cells were mixed in culture to control for background staining and then treated with 40 μM etoposide for 30 min or left untreated. The cells were fixed and RPA32 foci formation was detected by confocal microscopy. Arrows indicate shGLP cells. Ctr, no etoposide treatment. Scale bars: 10 μm.

Figure S4

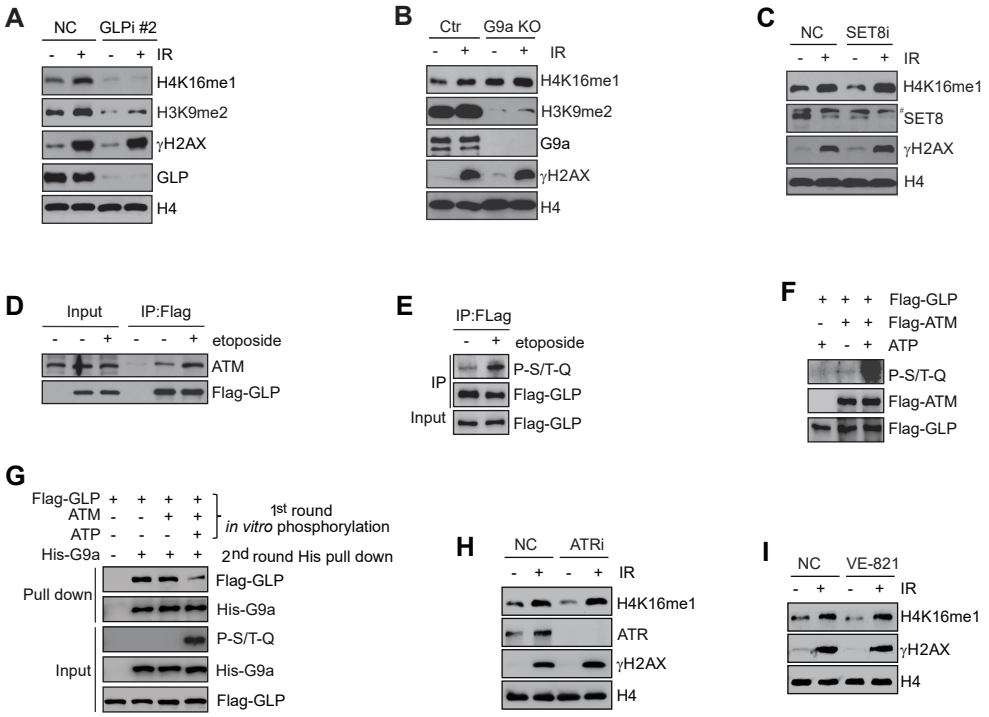
A
NC
GLPi #2
- + - + IR
H4K16me1
H3K9me2
γH2AX
GLP
H4
B
Ctr
G9a KO
- + - + IR
H4K16me1
H3K9me2
G9a
γH2AX
H4
C
NC
SET8i
- + - + IR
H4K16me1
SET8
γH2AX
H4
D
Input
IP:Flag
- - + - - + etoposide
ATM
Flag-GLP
E
IP:FLag
- + etoposide
IP
P-S/T-Q
Flag-GLP
Input
Flag-GLP
F
+ + + Flag-GLP
- + + Flag-ATM
+ - + ATP
P-S/T-Q
Flag-ATM
Flag-GLP
G
Flag-GLP + + + +
ATM - - + +
ATP - - - +
1st round
in vitro phosphorylation
His-G9a - + + + 2nd round His pull down
Pull down
Flag-GLP
His-G9a
Input
P-S/T-Q
His-G9a
Flag-GLP
H
NC
ATRi
- + - + IR
H4K16me1
ATR
γH2AX
H4
I
NC
VE-821
- + - + IR
H4K16me1
γH2AX
H4

Figure S4. GLP catalyzes H4K16me1 in response to DNA damage in an ATM-dependent manner.

(A) HCT116 cells were transfected with GLP siRNA#2 for 72 h before exposure to 10 Gy X-ray. The cells were then re-cultured for 30 min in fresh medium before protein extraction and western blotting with the indicated antibodies.

(B) G9a WT (Ctr) and G9a KO cells were treated with X-ray at 10 Gy. After 1 h, whole cell lysates and histones were extracted for western blotting.

(C) The same experiment described in (A) was performed with SET8 siRNA. #, non-specific bands.

(D) HCT116 cells were transfected with Flag-GLP for 2 d before 40 μM etoposide treatment for 30 min. Whole cell lysates were extracted and immunoprecipitated with anti-Flag M2 beads, and the interaction between GLP and ATM was assessed by western blotting.

(E) HCT116 cells were transfected with Flag-GLP for 2 d before 40 μM etoposide treatment for 30 min. Whole cell lysates were extracted and immunoprecipitated with an anti-Flag antibody, and the P-S/T-Q signal of GLP was assessed by western blotting.

(F) An *in vitro* phosphorylation assay was performed to check the activity of ATM towards GLP. Flag-GLP was purified from HCT116 cells, and ATM was immunoprecipitated from HCT116 cells and then incubated with GLP in phosphorylation reaction buffer [10 mM Tris-HCl (pH 7.4), 150 mM NaCl, 10 mM MgCl2, 0.5 mM DTT, 30 μM ATP] at 30 °C for 1 h.

(G) Flag-GLP and Flag-ATM were purified separately form G9a KO HCT116 cells and an *in vitro* phosphorylation assay was performed. Un-phosphorylated GLP or phosphorylated GLP was incubated with His-G9a in PBS (0.5% Triton X-100) at 4 °C for 3 h before His pull-down and detection by western blotting.

(H) HCT116 cells were transfected with ATR siRNA for 2 d and irradiated with X-ray at 10 Gy. After 30 min, chromatin bound fraction were extracted and detected by western blotting.

(I) HCT116 cells were pre-treated with 10 μM VE-821 for 4 h and irradiated with X-ray at 10 Gy. After 30 min, histones were extracted and detected by western blotting.

Figure S5

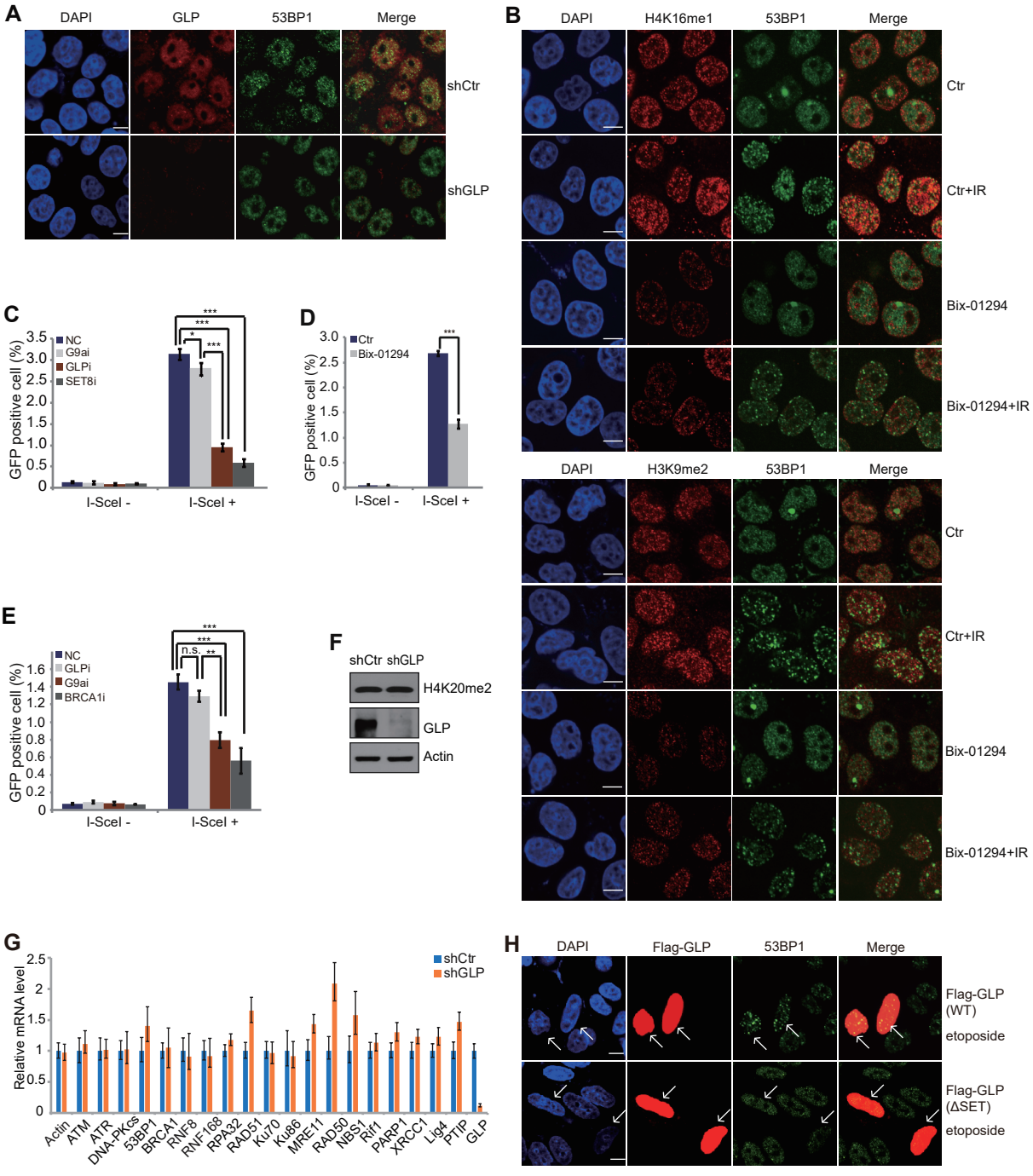
A
DAPI
GLP
53BP1
Merge
shCtr
shGLP
B
DAPI
H4K16me1
53BP1
Merge
Ctr
Ctr+IR
Bix-01294
Bix-01294+IR
DAPI
H3K9me2
53BP1
Merge
Ctr
Ctr+IR
Bix-01294
Bix-01294+IR
C
GFP positive cell (%)
NC
G9ai
GLPi
SET8i
I-SceI -
I-SceI +
D
GFP positive cell (%)
Ctr
Bix-01294
I-SceI -
I-SceI +
E
GFP positive cell (%)
NC
GLPi
G9ai
BRCA1i
n.s.
I-SceI -
I-SceI +
F
shCtr shGLP
H4K20me2
GLP
Actin
G
Relative mRNA level
shCtr
shGLP
Actin
ATM
ATR
DNA-PKcs
53BP1
BRCA1
RNF8
RNF168
RPA32
RAD51
Ku70
Ku86
MRE11
RAD50
NBS1
Rif1
PARP1
XRCC1
Lig4
PTIP
GLP
H
DAPI
Flag-GLP
53BP1
Merge
Flag-GLP (WT) etoposide
Flag-GLP (ΔSET) etoposide

Figure S5. GLP regulates NHEJ by targeting 53BP1.

(A) Representative images showing GLP expression and 53BP1 foci formation in the experiment described in Figure 4E. Similar results were observed in at least three independent experiments.

(B) HeLa cells were pre-treated with or without 2.5 μM Bix-01294 for 24 h before X-ray irradiation. Cells were fixed and stained with anti-H4K16me1 and anti-53BP1 antibodies (upper panels) or stained with anti-H3K9me2 and anti-53BP1 antibodies (lower panels).

(C) NHEJ efficiency following G9a, GLP or SET8 siRNA-mediated knockdown. A pool of GLP siRNA#1 and #2 was used. "NC" indicates the scrambled siRNA used as a negative control. The data represent the means ± SD, *$p < 0.05$, ***$p < 0.001$ (Student's *t*-test).

(D) NHEJ efficiency following treatment with 2.5 μM Bix-01294 for 24 h. Three independent experiments were performed. The data represent the means ± SD, ***$p < 0.001$ (Student's *t*-test).

(E) HR efficiency following GLP, G9a or BRCA1 siRNA-mediated knockdown in DR-U2OS cells. A pool of GLP siRNA#1 and #2 was used. "NC" indicates the scrambled siRNA used as a negative control. The data represent the means ± SD, n.s., not significant, **$p < 0.01$, ***$p < 0.001$ (Student's *t*-test).

(F) Western blot analysis of H4K20me2, GLP and Actin in shCtr and shRGLP cells.

(G) mRNA levels of DNA repair factors in shCtr and shGLP cells.

(H) shGLP cells were transfected with reconstituted Flag-GLP (WT) or Flag-GLP (ΔSET) for 72 h and then treated with 40 μM etoposide for 30 min. The cells were then fixed and immunostained with anti-Flag and anti-53BP1 antibodies. Arrows indicate successfully transfected cells. Ctr, no etoposide treatment. Scale bars: 10 μm.

Figure S6

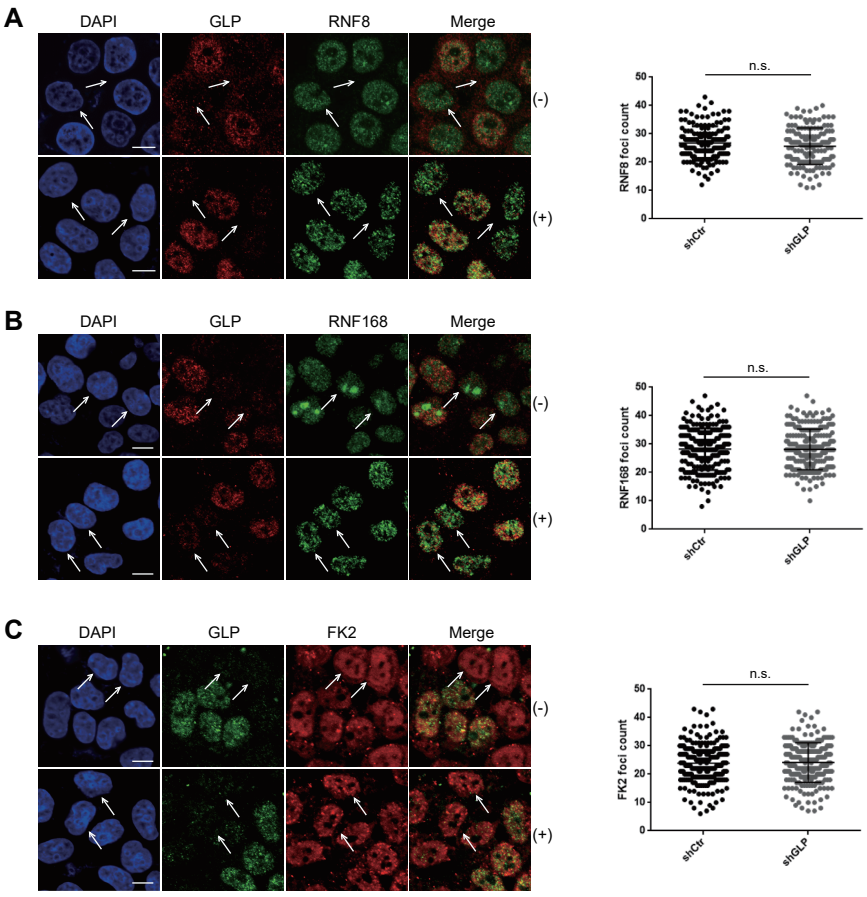
A
DAPI
GLP
RNF8
Merge
(-)
(+)
n.s.
RNF8 foci count
shCtr
shGLP
B
DAPI
GLP
RNF168
Merge
(-)
(+)
n.s.
RNF168 foci count
shCtr
shGLP
C
DAPI
GLP
FK2
Merge
(-)
(+)
n.s.
FK2 foci count
shCtr
shGLP

Figure S6. Foci formation of RNF8, RNF168 and FK2 in control and GLP-deficient cells

(A-C) shCtr and shGLP HeLa cells were mixed in culture to control for staining background and then treated with 40 μM etoposide for 30 min or left untreated. The cells were fixed and RNF8 (A), RNF168 (B) and FK2 (C) foci formation was detected by confocal microscopy. Arrows indicate the shGLP cells. (-), no etoposide treatment. (+), etoposide treatment. Scale bars: 10 μm. Representative images are shown on the left. Calculations from at least 200 cells are shown on the right. The data represent the means ± SD. n.s., not significant. Consistent results were obtained from at least three different experiments.

Figure S7

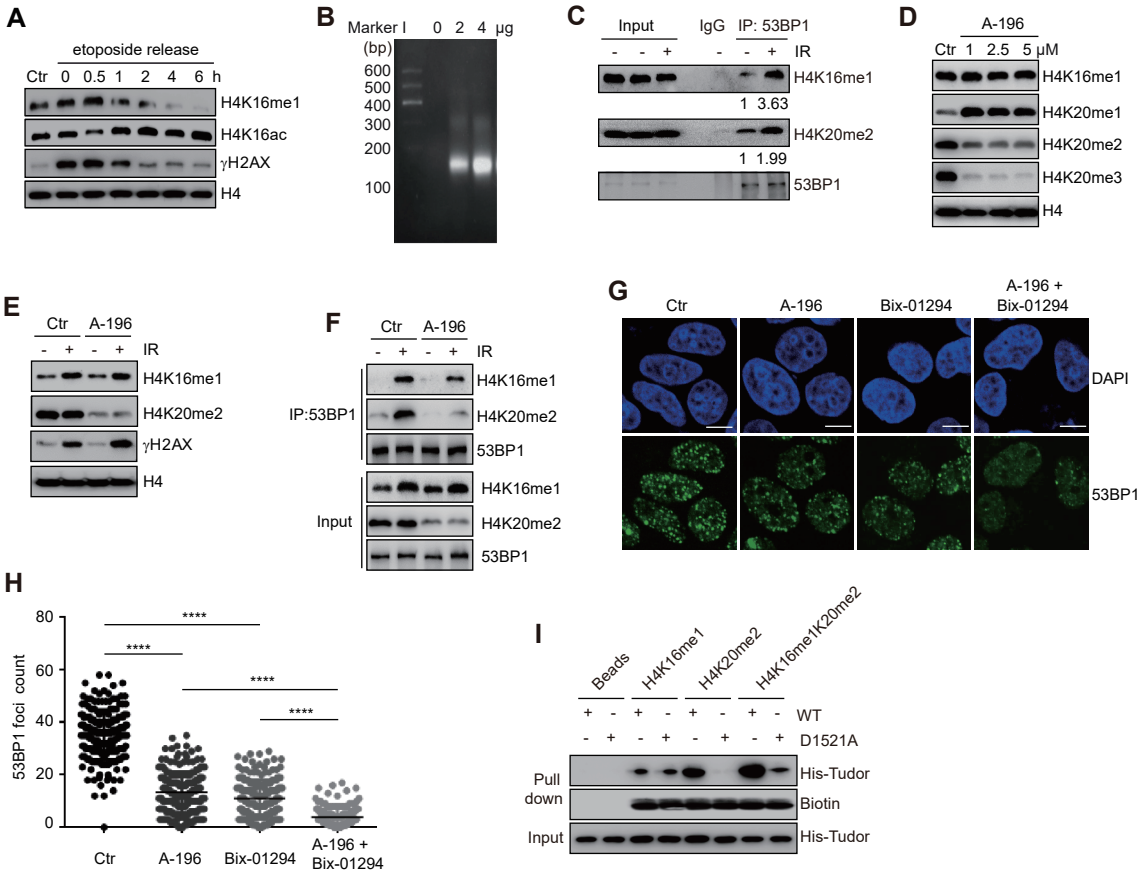
A
etoposide release
Ctr 0 0.5 1 2 4 6 h
H4K16me1
H4K16ac
γH2AX
H4
B
Marker I 0 2 4 μg
(bp)
600
500
400
300
200
100
C
Input
IgG
IP: 53BP1
IR
H4K16me1
1 3.63
H4K20me2
1 1.99
53BP1
D
A-196
Ctr 1 2.5 5 μM
H4K16me1
H4K20me1
H4K20me2
H4K20me3
H4
E
Ctr
A-196
IR
H4K16me1
H4K20me2
γH2AX
H4
F
Ctr
A-196
IR
IP:53BP1
H4K16me1
H4K20me2
53BP1
Input
H4K16me1
H4K20me2
53BP1
G
Ctr
A-196
Bix-01294
A-196 +
Bix-01294
DAPI
53BP1
H
53BP1 foci count
80
60
40
20
0
****
****
****
****
Ctr
A-196
Bix-01294
A-196 +
Bix-01294
I
Beads
H4K16me1
H4K20me2
H4K16me1K20me2
WT
D1521A
Pull
down
His-Tudor
Biotin
Input
His-Tudor

Figure S7. H4K16me1 cooperates with H4K20me2 for 53BP1 recruitment in the DDR.

(A) HCT116 cells were treated with 40 μM etoposide for 30 min. The cells were then washed four times with PBS and re-cultured in fresh medium. Histones were then extracted at each release time (indicated) and analyzed by western blotting.

(B) The efficiency of mononucleosome extraction was assessed by electrophoresis of the DNA extracted from obtained mononucleosomes.

(C) HCT116 cells were treated with 10 Gy X-ray irradiation and re-cultured for 30 min. The chromatin fractions were extracted for anti-53BP1 immunoprecipitation. The interacted histones were analyzed by western blotting.

(D) HCT116 cells were treated with A-196 at indicated concentration for 2 d before histone extraction and western blotting.

(E) HCT116 cells were pre-treated with 2.5 μM A-196 for 2 d and irradiated with X-ray at 10 Gy. After 30 min, histones were extracted and analyzed by western blotting.

(F) HCT116 cells were pre-treated with 2.5 μM A-196 for 2 d and irradiated with X-ray at 10 Gy. Whole cell lysates were extracted for anti-53BP1 Co-IP. The interacted histones were analyzed by western blotting.

(G-H) Hela cells were pre-treated with 2.5 μM A-196 or 2.5 μM Bix-01294 respectively for 2 d, or pre-treated with a combination of 2.5 μM A-196 and 2.5 μM Bix-01294 for 2d and then subjected to 10 Gy X-ray irradiation. After 20 min, cells were fixed and stained with anti-53BP1 antibody. 53BP1 foci formation was detected by confocal microscopy. Consistent results were observed from three independent experiments. Representative confocal images are shown in (G). Calculations from at least 200 cells per sample are shown in (H). The data represent the means ± SD, ****$p<0.0001$ (Student's *t*-test).

(I) A peptide pull-down assay was performed to monitor the interactions between His-Tudor WT or His-Tudor D1521A with the indicated peptides.

Figure S8

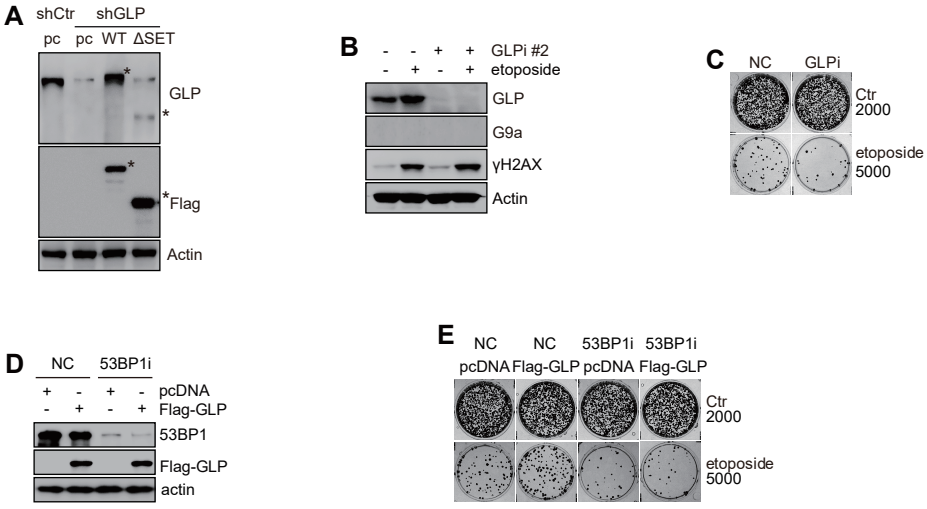
A
shCtr
shGLP
pc
pc
WT
ΔSET
GLP
Flag
Actin
B
GLPi #2
etoposide
GLP
G9a
γH2AX
Actin
C
NC
GLPi
Ctr
2000
etoposide
5000
D
NC
53BP1i
pcDNA
Flag-GLP
53BP1
Flag-GLP
actin
E
NC
NC
53BP1i
53BP1i
pcDNA
Flag-GLP
pcDNA
Flag-GLP
Ctr
2000
etoposide
5000

Figure S8. GLP-catalyzed H4K16me1 is important for cell survival after DNA damage.

(A) Western blots showing endogenous GLP expression in shCtr and shGLP cells and exogenously re-expressed GLP in shGLP cells.

(B) Western blots showing endogenous GLP knockdown in the experiment performed in Figure 6F.

(C) Representative images for the colony formation assay performed in Figure 6F. Consistent results were observed from three independent experiments.

(D) Western blots showing endogenous 53BP1 knockdown and Flag-GLP over-expression in the experiment performed in Figure 6G.

(E) Representative images for the colony formation assay performed in Figure 6G. Consistent results were observed from three independent experiments.

Table S1. The primers used in RT-PCR assays.

Ku70-F	TTGCTTCTGCCTAGCGATACC
Ku70-R	AAACCTGGATCATCAAACCGTT
RNF168-F	GACCGTCGAAAAGGCGAGTT
RNF168-R	TTGACGAGAGAATTTCTTCGGG
Ku86-F	GCACTGACAATCCCCTTTCTG
Ku86-R	TCAATGTCCTCCAGCAAATCAAA
XRCC1-F	TCAAGGCAGACACTTACCGAA
XRCC1 -R	TCCAACTGTAGGACCACAGAG
Actin-F	CCAACCGCGAGAAGATGA
Actin-R	CCAGAGGCGTACAGGGATAG
ATM-F	ATCTGCTGCCGTCAACTAGAA
ATM-R	GATCTCGAATCAGGCGCTTAAA
ATR-F	TCCCTTGAATACAGTGGCCTA
ATR-R	TCCTTGAAAGTACGGCAGTTC
DNAPK-cs-F	CTGTGCAACTTCACTAAGTCCA
DNAPK-cs-R	CAATCTGAGGACGAATTGCCT
RNF8-F	CCCGGCTTCTTCGTCACAG
RNF8-R	ACCTCGCACCCATCTTCCA
Lig4-F	GAACGTATGCAAATGCACAAAGA
Lig4-R	ACCTTCAGTAGGAGAAGCACC
53BP1-F	TGAGCAGTTACCTCAGCCAAA
53BP1-R	AAGGGAATGTGTAGTATTGCCTG
RAD51-F	CAACCCATTTCACGGTTAGAGC
RAD51-R	TTCTTTGGCGCATAGGCAACA
PTIP-F	ACAATGCACTAGCCTCACACA
PTIP-R	ACACTGAACGGACAGAATCAC
RPA32-F	GCTGTCTTGGGTGCATTGGA
RPA32-R	GCATGATCTTAAAGGCTACCAGG
RIF1-F	GCACAAAAGGTACATTTGCGG
RIF1-R	AGCTGCTCCGTAATAGATGCT
MRE11-F	GGGGCAGATGCACTTTGTG
MRE11-R	GAAGCAAAACCGGACTAATGTCT
RAD50-F	TTTGGTTGGACCCAATGGGG
RAD50-R	CAGGAGGGAAATCTCCAGTACAA
NBS1-F	CACTCACCTTGTCATGGTATCAG
NBS1-R	CTGCTTCTTGGACTCAACTGC
BRCA1-F	GAAACCGTGCCAAAAGACTTC
BRCA1-R	CCAAGGTTAGAGAGTTGGACAC
PARP1-F	TGGAAAAGTCCCACACTGGTA
PARP1-R	AAGCTCAGAGAACCCATCCAC
GLP-F	CATGCAGCCAGTAAAGATCCC
GLP-R	CTGCTGTCGTCCAAAGTCAG